Bioresource Technology 274 (2019): 395-402

DOI: https://doi.org/10.1016/j.biortech.2018.11.103

Valorization of microalgal biomass by hydrothermal carbonization and anaerobic digestion

J.D. Marin-Batista, J.A. Villamil, J.J. Rodriguez, A.F. Mohedano, M.A. de la Rubia*

Chemical Engineering Department, Universidad Autonoma de Madrid, Campus de Cantoblanco, 28049, Madrid, Spain.

angeles.delarubia@uam.es

Abstract

The potential of hydrothermal carbonization (HTC) as a novel choice for treating microalgal biomass (MAB) was assessed. The hydrochar obtained at 210 ºC had a carbon content and a higher heating value (HHV) 1.09 and 1.1 times greater, respectively, than that of the feedstock. Also, washing the hydrochar with HCl efficiently removed ash and increased its carbon content 1.40-fold. Energy recovery in the liquid fraction from the hydrothermal treatment (LF) by anaerobic digestion (AD) allowed methane yields of 188–356 mL STP CH_4 g^{-1} VS_{added}, to be obtained. As a result, the amount of energy recovered from MAB was increased from about 4 MJ kg^{-1} (20% in terms of HHV) to 15.4, 12.1 and 10.4 MJ kg^{-1} by combining HTC at 180, 210 and 240 ºC, respectively, with AD. Therefore, HTC at 180 ºC in combination with AD seemingly provides an effective method for valorizing MAB.

Keywords: anaerobic digestion; energy recovery; hydrochar; hydrothermal carbonization; microalgae.

1. Introduction

Microalgal biomass (MAB) is widely accepted as a competitive feedstock for biofuel production on the grounds of its high growth rate (biomass doubling time < 3.5 h), high productivity (up to 26 300 t km^{-2} yr^{-1} on a dry basis, and high content in valuable compounds such as carbohydrates (7–69%), proteins (15–84%) and lipids (1–63%) (Xia et al., 2013; Barbera et al., 2018). Although MAB has a highly promising potential as a renewable energy source, developing an efficient microalgal biofuel production process remains a tough challenge owing to the high cost of biomass production in terms of supply of nutrients (especially nitrogen and phosphorus) and auxiliary energy inputs in downstream processes (Fasaei et al., 2018). Integrating microalgal cultivation systems based mainly on pound raceways and photobioreactors with wastewater treatments has become a promising choice to reduce nutrient requirements for biomass production (Gouveia et al., 2016). In fact, microalgae can recover 82–92% of nitrogen and 58–98% of phosphorus, and remove up to 62% of chemical oxygen demand (COD), from wastewater (Hernández et al., 2013; Lee et al., 2016). Even though using wastewater as a culture medium has boosted the economic viability of microalgal biofuels, mass balances and resource assessments have shown that wastewater cannot fulfil by itself the nutrient requirements for large-scale production (Shurtz et al., 2017). Producing nutrient recycling streams during downstream processing of microalgal biomass is in fact crucial to develop a cost-effective, environmentally sustainable route for its production (Barbera et al., 2018).

Downstream processing of microalgal biomass for biofuel production remains a bottleneck because valuable compounds contained in the biomass (particularly carbohydrates, lipids, and proteins) are located inside cells (Ho et al., 2013). Indeed, cell walls in microalgae contain non-hydrolysable biopolymers termed “algeanans” that have often been deemed refractory to biological degradation (Ras et al., 2011). Research in this area has thus focused on valorizing microalgal biomass by extracting valuable compounds to increase biofuel conversion yields and then subjecting extracted microalgal

residues to anaerobic digestion (AD) in order to cycle nutrients and recover additional energy from biogas (Ayala-Parra et al., 2017; Delrue et al., 2012; Guldhe et al., 2014). However, this valorization route is of limited efficiency because MAB contains more than 80% moisture and thus requires drying to enable extraction (Chiaramonti et al., 2017). The target final moisture content of most applications, 10%, requires using too much energy with conventional drying methods (Hosseinizand et al., 2017). A conversion process directly converting wet microalgal biomass into refinery intermediates for subsequent upgrading to commercial fuels is therefore needed (Costanzo et al., 2015).

One such conversion technology is hydrothermal carbonization (HTC), which uses milder temperatures (around 200 ºC) than other hydrothermal processes such as hydrothermal liquefaction (280–370 ºC) or hydrothermal gasification (400–700 ºC) (Yao et al., 2016). During HTC, wet biomass provides both the reactant and the medium for a complex series of reactions including dehydration, decarboxylation and demethanation that lower O/C and H/C atomic ratios in the feedstock, thereby resulting in a more energy-dense slurry (Smith et al., 2018; Yu et al., 2014) consisting of a solid fraction and a liquid fraction. The solid fraction is a hydrochar (HC), some properties of which such as higher heating value (HHV) and fuel ratio can be improved to obtain a valuable material for co-firing with coal or for safe disposal as a soil amendment on agricultural land (Santos and Pires, 2018). The liquid fraction (LF) contains large concentrations of COD (90–100 g L^{-1}) and TKN (8.7 g N L^{-1}) derived from refractory compounds produced in the HTC reaction (e.g., oxygen-containing aromatic compounds such as phenols and furans, and nitrogen-containing compounds such as pyrazines and aromatic amines) (Villamil et al., 2018). Although the methane yields obtained by anaerobic digestion of the liquid fraction can be influenced by the presence of nitrogen-containing species, the treatment usually allows almost complete removal of furan and partial removal of phenol species to an extent depending on the origin of the material and the inoculum concentration (De la Rubia et al., 2018a).

Although the optimal configuration for a microalgal biorefinery based on a hydrothermal treatment has been widely discussed, no consensus has to date been reached (López Barreiro et al., 2014). HTC processing of microalgae can be approached mainly in three different ways. One involves directly using raw microalgal biomass of, for example, *Chlorella vulgari*s or *Chlamydomonas reinhardtii* for HTC to assess hydrochar mass yield, chemical composition and solid-fuel properties at different temperatures and reaction times (Heilmann et al., 2010; Park et al., 2018). Another approach previously extracts lipids from microalgal cells (e.g., *C. vulgaris, Spirulina* spp.) and then converts lipid-extracted microalgae into hydrochar at different temperatures in order to obtain solid fuel with the best possible properties (Lee et al., 2018). The liquid fractions provided by the previous two approaches have been assessed for recovery of highly valuable chemicals such as sugars, alcohols and volatile fatty acids (Broch et al., 2014), and for nutrient (N and P) recycling with a view to producing microalgal biomass (Yao et al., 2016). The third approach involves a post-treatment scenario where anaerobic digestion (AD) is directly used as the primary treatment to remove the biodegradable fraction from microalgal biomass (*Scenedesmus* spp.), whereas the resulting digestate is hydrothermally treated to degrade particulate organic fraction by recycling the liquid fraction through the digester (Nuchdang et al., 2018).

In this work, we used the first approach to assess the influence of temperature on HTC byproducts (hydrochar and liquid fraction) of microalgal biomass. Despite the potential of HTC for valorizing microalgae, the fundamental energy balances of integrated HTC–AD processing remain unknown. A sound knowledge of the balances is crucial with a view to assessing the potential sustainability of the overall biofuel production process. This led us to conduct batch AD tests on the liquid fraction from the hydrothermal treatment of microalgal biomass in order assess methane yields and biodegradability of refractory compounds.

2. Materials and Methods

2.1. Hydrochar production

HTC tests were performed at 180, 210 and 240 ºC in an electrically heated 4 L ZipperClave® pressure vessel. The vessel was loaded with 2 kg on wet basis (98%) of microalgal biomass containing (65.9 ± 3.5) g L^{-1} total solids (TS), (57.9 ± 2.5) g L^{-1} volatile solids (VS) and (109.0 ± 5.7) g L^{-1} total chemical oxygen demand (TCOD). This feedstock was obtained from the Food Innovation and Sustainability Center in Almeria, Spain, and cultured outdoors in a thin-layer photobioreactor (1200 L working volume, 33 m^2 surface area) that was fed with 10% diluted centrifuged pig manure (PM) at a hydraulic retention time (HRT) of 0.3 d and discretely centrifuged on a GEA centrifuge (Westphalia, Germany) (Hernandez et al., 2018). The operating temperature for the HTC runs was reached by heating at a rate of 3 ºC min^{-1} and then held for 1 h. The reaction was stopped by cooling with an internal heat exchanger using tap water. The slurry thus obtained (hydrochar and liquid fraction) was centrifuged on a SIGMA 3-16L centrifuge equipped with a fixed angle rotor (cod. 12159). The hydrochar was obtained by oven-drying the solid fraction overnight at 105 ºC, and then ground and sieved. A Filtra No. 38373 sieve was used to shred the hydrochar into three particle size ranges, namely: $\emptyset >$ 0.5 mm; 0.25 < $\emptyset$ < 0.5 mm and $\emptyset$ < 0.25 mm, the last fraction being used for characterization. The liquid fraction was recovered by passage through a 0.45 μm filter and stored at 4 ºC for use as substrate in the anaerobic digestion tests.

The three hydrochars obtained were labelled HC180, HC210, and HC240. Inorganic compounds on the surface of HC210 were removed by washing with three different solvents, namely: 96% ethanol (4 mL g^{-1} hydrochar), 1 M HCl (50 mL g^{-1} hydrochar) and 3% (v/v) H_2O_2 (50 mL g^{-1} hydrochar). Extraction was performed with each of the three solvents for 2 h in a Soxhlet extractor (total extraction time, 6 h), the resulting extracts being dried in an oven at 105 ºC for 24 h.

139 *2.2. Anaerobic digestion inoculum*

140 The inoculum used in the anaerobic batch tests was granular anaerobic sludge from an
141 industrial digester processing brewery wastewater under mesophilic conditions (35 ºC).
142 The inoculum characteristics were as follows: pH 7.6 ± 0.1, 57.5 ± 1.4 g TS L^{-1}, 46.3 ±
143 1.7 g VS L^{-1}, 70.7 ± 1.7 g O_2 L^{-1} of total COD (TCOD) and 0.3 ± 0.1 g O_2 L^{-1} of soluble
144 COD (SCOD).

145

146 *2.3. Batch anaerobic tests*

147 Anaerobic digestion runs were carried out in 120 mL glass serum vials. The initial
148 inoculum concentration was set at 15 g VS L^{-1} and the inoculum-to-substrate ratio (ISR)
149 at 2:1 on a VS basis. A basal medium containing macro- and micronutrients that was
150 prepared and dosed as described elsewhere (Villamil et al., 2018) was added, after which
151 the vial was made to volume (60 mL) with distilled water. The reaction medium was
152 flushed with N_2 for 3 min in order to ensure anaerobic conditions. Then, the vials were
153 sealed with rubber stoppers and metallic crimps, and held in a thermostated water bath at
154 mesophilic temperature [(35 ± 1) ºC] with shaking at 80 rpm.

155

156 The time course of anaerobic digestion was followed by using 10 vials at each
157 temperature studied. Seven of them were sacrificed: two during the first three days and
158 then every week. The remaining three vials were used for biogas analysis (volume and
159 composition) only. Triplicate blank samples containing no substrate were also used to
160 establish the background biogas level from the inoculum, and so were triplicate starch
161 positive controls (Panreac) that yielded (341 ± 10) mL STP CH_4 g^{-1} COD_{added}
162 [approximately 97% of the theoretical specific yield (350 mL CH_4 g^{-1} COD_{added})] to
163 confirm that the inoculum was active. Specific methane production (SMP) was calculated
164 by subtracting the amount of methane produced by the blanks from the amount of
165 methane production exceeding the initial VS_{added} value for each substrate in each batch
166 reactor.

167

168 *2.4. Analytical methods*

169 The elemental composition of the solid samples (C, H, N and S) was determined on a
170 CHNS analyzer (LECO CHNS-932, Model601-800-500), using the manufacturer's
171 standard procedures. A proximate analysis was done by thermogravimetric analysis
172 (TGA) according to ASTM D7582 in order to determine moisture, ash and volatile matter
173 (VM). Elements were quantified by inductively coupled plasma atomic emission
174 spectroscopy (ICP-MS) on an Elan 6000 Sciex instrument from Perkin Elmer. The HHV
175 of dried solid samples were determined by using an IKA C2000 calorimetric bomb
176 according to technical specification UNE-EN 5400. Table 1 summarizes the
177 characteristics of the MAB and hydrochars.

178

179 The raw feedstock (MAB) and the inoculum were characterized by measuring pH with a
180 Crison 20 Basic pH-meter, TS and VS according to standard method 2540B and 2540E,
181 respectively (APHA, 1998), and TCOD according to Raposo et al. (2008). As regards
182 soluble samples, MAB and sacrificed samples from the anaerobic digestion tests were
183 centrifuged and passed through a filter of 0.45 μm pore size, whereas the initial liquid
184 fractions (LF180, LF210 and LF240) were analyzed for SCOD by using standard method
185 5220D (APHA, 1998); total organic carbon (TOC) on a Shimadzu TOC–VCPN
186 autoanalyser; carbohydrates according to Dubois et al. (1956); proteins with the Lowry
187 method (Randall and Lewis, 1951); pH and total alkalinity by titration to pH 4.3 with 0.02
188 N H_2SO_4; and total ammonia nitrogen (TAN) by distillation and titration according to
189 standard method 4500E (APHA, 1998). The concentrations of individual volatile fatty
190 acids (VFAs) from acetic to heptanoic, iso-forms included, were determined by gas
191 chromatography (GC) on a Varian 430-GC instrument equipped with a flame ionization
192 detector (FID) and a capillary column filled with Nukol (nitroterephthalic acid-modified
193 polyethylene glycol). Chemical species were identified by GCy/ion trap mass
194 spectrometry (GC–MS) on a CP-3800/Saturn 2200 instrument equipped with a Varian
195 CP-8200 autosampler injector and a Carbowax/Divinyl benzene Yellow Green solid-
196 phase micro-extractor, and furnished with a Factor Four VF-5 MS capillary column (30

m long, 0.25 mm i.d.) (de la Rubia et al., 2018b). Compounds were identified against the NIST 2008 Library. Biogas production was assessed manometrically (Rozzi and Remigi, 2004) by measuring the pressure increase in each vial with an electronic pressure monitor (ifm, PN7097). The amount of biogas was expressed under standard temperature and pressure conditions (273 K and 1 bar). Finally, the gas composition (H_2, CO_2 and CH_4) was determined on a Thermo Scientific Trace 177 1310 GC (de la Rubia et al., 2018b).

2.5. Data processing and analysis

2.5.1. Product yield

Product mass yields were calculated from Eq. (1). Hydrochar mass yield (Y_{HC}) was defined as the weight ratio of recovered hydrochar (W_{HC}) to microalgal feedstock (W_{MAB}) on a dry basis. Similarly, the liquid-fraction mass yield (Y_{LF}) was taken to be the weight ratio of recovered liquid fraction (W_{LF}) to microalgal biomass fed (W_{MAB}), also on a dry basis.

$$Y_{HC,LF}(\%) = \left(W_{HC,LF}/W_{MAB}\right) \cdot 100 \quad (1)$$

2.5.2. Higher heating value of the liquid fraction

The specific methane yields obtained in the batch anaerobic tests were converted into HHV values by using the following equation:

$$HHV_{LF}(MJ/kg) = 39.8 \cdot 10^{-3} \cdot SMY \cdot (VS/TS) \quad (2)$$

where SMY denotes specific methane yield and VS/TS the ratio of VS to TS added to the anaerobic reactors with each substrate. The coefficient $39.8 \cdot 10^{-3}$ is the lower heating value for pure methane in MJ N^{-1} m^{-3}.

2.5.3. Energy recovery

The energy yield of the hydrochars and methane were calculated from the following equation:

$$Energy\ yield_{HC,LF}(\%) = (HHV_{HC,LF}/HHV_{MAB}) \cdot Y_{HC,LF} \quad (3)$$

where HHV_{HC} (MJ kg^{-1}) is HHV for each hydrochar, HHV_{LF} that for each liquid fraction as calculated from eq. (2) and HHV_{MAB} that for the microalgal biomass. $Y_{\mathrm{HC,LF}}$ denotes the mass yield of each hydrochar (Y_{HC}) or that of the liquid fraction (Y_{LF}). The net energy recovery was assumed to be the combination of Y_{HC} and Y_{LF}.

3. Results and Discussion

3.1. Hydrochar properties

Hydrochar yield (eq. 1) decreased slightly with increasing temperature and was close to 37% for all HCs. A representative analysis of MAB and hydrochars is shown in Table 1. Carbon content was similar for HC180 and HC210, but somewhat lower for HC240 as a result of carbon bond breakage on the surface of the material, and of the release of carbon as CO and CO_2, at relatively high temperatures (Lee et al., 2018). Therefore, a large fraction of carbon in the feedstock was transferred to the aqueous phase under severe reaction conditions. The hydrogen and oxygen contents decreased with increasing HTC temperature through chemical dehydration and decarboxylation. Likewise, the nitrogen content decreased with increasing severity of the hydrothermal treatment (to 2.3% at the highest temperature studied). On the other hand, the sulfur content was similar and close to 0.1% for all hydrochars. Also, as previously found by Park et al. (2018) in *Chlorella vulgaris* and Heillman et al. (2010) in various microalgal species, the nitrogen and sulfur contents of the hydrochars were lower than those of the feedstock. Therefore, low sulfur and nitrogen contents may result in scant formation of SO_x and NO_x species through hydrochar combustion (Engin et al., 2018).

Table 1 also shows the amounts of volatile matter (VM) and fixed carbon (FC) present in the hydrochars, and their HHVs. A high VM content in solid fuel may result in flame instability during combustion and hence in excessive heat loss. In addition, a high FC content increases the firing temperature and can thus help to maintain a steady, less violent flame. The fuel ratio (FC/VM) has been used to rank hydrochars as effective alternative coal-based fuels (He et al., 2013). In our hydrochars, FC/VM increased

gradually from 0.2 to 0.4 by effect of FC increasing and VM decreasing with increasing HTC temperature. HHV for the feedstock was 16.9 MJ kg^{-1}, which is similar to the value reported by Park et al. (2018) for *Chlorella vulgaris* (16.5 MJ kg^{-1}). HHV increased with increasing temperature except at 240 ºC, which is consistent with the carbon loss observed at a relatively high HTC temperature. Consequently, raising the HTC temperature affected energy production —and fuel properties as a result. The HHVs for the hydrochars obtained from MAB are comparable to those for lignite (Engin et al., 2018). Park et al. (2018) obtained greater HHVs for hydrochars from the hydrothermal treatment of *Chlorella vulgaris* at temperatures similar to ours (180−240 °C), 24.8–29.8 MJ kg^{-1}, and Heilmann et al. (2010) reported HHVs of 30.5 and 31.6 MJ kg^{-1} for *Dunaliella salina* and *Chlamydomonas reinhardtii*, respectively, hydrothermally treated at 200 ºC for 2 h. It should be noted that the physicochemical properties of hydrochars are strongly dependent on the composition of the raw material. Most reported results were obtained with pure microalgal cultures that have not been used in wastewater treatments. Moreover, our HTC treatment was intended for use as a valorization method.

Figure 1 shows a van Krevelen diagram. The variation of the O/C and H/C atomic ratios allows estimating the degree of deoxygenation of biomass by decarboxylation or dehydration. Low O/C and H/C ratios are needed to avoid energy losses in combustion fumes and steam (Missaoui et al., 2017). The degree of carbonization resulting from the HTC treatment was similar at 210 and 240 ºC. Figure 1 includes the typical zones for biomass, peat, lignite, sub-bituminous and bituminous materials, and anthracite. As can be seen, the O/C and H/C ratios for raw MAB decreased to levels typical of lignite as the HTC temperature was raised. As previously found by Park et al. (2018) in the HTC of *Chlorella vulgaris* microalgae over the temperature range 150–270 ºC, MAB conversion in this work occurred essentially through dehydration. This conclusion was confirmed by the proximate analysis (Table 1), which revealed that the fuel properties of the resulting hydrochars were consistent with those of low-grade lignite as reported by Engin et al. (2018).

283

284 In an attempt to increase the C content, various solvents to remove ash and byproducts
285 from their surface were tested (Table 2). Whereas ethanol and H_2O_2 failed to improve the
286 elemental composition of the hydrochars, HCl efficiently removed ash and soluble
287 compounds, thereby increasing their HHVs by a factor of 1.37 and making them usable
288 as solid fuels. The high complexity of the chemical routes involved will require further
289 research to identify the particular species removed in the process.

290

291 Figure 2 shows the distribution of elements in the feedstock and hydrochars. Except for
292 Na and K, the element contents of the hydrochars increased with increasing temperature.
293 Ekpo et al. (2016) previously observed a similar trend with increasing reaction severity
294 in the HTC treatment of *Chlorella vulgaris*; however, Na and K contents also increased
295 with increase in reaction temperature. The Ca content of our hydrochars, (54.0 ± 1.2) mg
296 g^{-1}, is much higher than that reported by Ekpo et al. (2016): 16.8 mg g^{-1}. The difference
297 can ascribed to the origin of our MAB, which was fed with pig manure rich in mineral
298 matter (Hernández et al., 2018); also, the difference reflected in a high ash content in the
299 hydrochars (Table 1). Phosphorus content, which is a highly valuable byproduct for use
300 in a number of fertilizers, increased by a factor of 1.8 upon hydrothermal treatment at 240
301 ºC, but remained at its initial level with the treatment at 180 ºC.

302

303 *3.2. Characterization of the liquid fraction from hydrothermal carbonization*

304 Increasing the HTC temperature slightly reduced the concentrations of total and volatile
305 solids from the raw MAB to the liquid fractions. Thus, 52.8 and 58.3% of the initial
306 amount of TS and VS, respectively, remained in LF180 (Table 3). By contrast,
307 temperatures above 180 ºC considerably reduced TS and VS (to 38.1 and 39.9%,
308 respectively, in LF240). An increase in SCOD was also observed. In fact, SCOD in MAB
309 accounted for only 2.5% of TCOD but increased eight-fold upon hydrothermal treatment
310 (from 2.5 g L^{-1} to 22.3–26.8 g L^{-1} in the liquid fractions). This result can be ascribed to
311 (*a*) disruption or hydrolysis of the microalgal cell envelope during the hydrothermal

312 treatment increasing the concentrations of intracellular soluble compounds such as
313 carbohydrates and proteins (Wang et al., 2018); and (*b*) reaction of soluble compounds
314 with intermediates formed during the HTC process (Funke and Ziegler, 2010). pH and
315 total alkalinity related to TVFA and ammonia nitrogen were also influenced by increased
316 HTC temperatures (Aragon-Briceño et al., 2017). A similar trend was observed in TOC,
317 which increased 5 times with respect to the initial concentration in the soluble fraction of
318 MAB.
319
320 *3.3. Anaerobic digestion of the liquid fraction*
321 pH, TA and TAN (results not shown) in anaerobic digestion processes are closely related.
322 The initial pH in the batch tests on MAB and the liquid fractions obtained by HTC at 180,
323 210 and 240 ºC ranged from 8.2 to 8.5; also, pH remained at 7.5–7.8 during the anaerobic
324 process. TA was initially less than 2500 mg $CaCO_3$ L^{-1} but increased to 3450–5800 mg
325 $CaCO_3$ L^{-1} in all runs. pH and TA were more than adequate for buffering purposes and
326 hence for anaerobic digestion (Appels et al., 2008; de la Rubia et al., 2018a). The initial
327 TAN value increased with increasing temperature because of total nitrogen being
328 redistributed into various byproducts during the HTC treatment (Wang et al. 2018). Thus,
329 the lowest initial TAN value, (308 ± 1 mg L^{-1}), was obtained with raw MAB, whereas
330 the highest, (672 ± 2 mg L^{-1}), was provided by LF240. The final TAN value ranged from
331 630 ± 2 to 1456 ± 5 mg L^{-1}, and was thus below the ammonia inhibition threshold: 1.7 g
332 L^{-1} (Villamil et al., 2019). Therefore, no ammonia toxicity, which is one of the limiting
333 factors for anaerobic digestion of MAB (Ras et al., 2011), was observed; also, only LF240
334 approached the inhibiting value.
335
336 Methanogenic microorganisms use SCOD (Fig. 3a) in the form of VFA (Fig. 3b) for
337 methane production (Fig. 3c). Therefore, the time course of SCOD and VFA can provide
338 useful information about the performance of the different stages of anaerobic digestion,
339 namely: hydrolysis and acidogenesis from SCOD, and acidogenesis and methanogenesis
340 through TVFA. Fig. 3a illustrates the effect of the HTC temperature on SCOD removal

341 from the liquid fractions (LFs). SCOD was removed by 51 and 44% from LF180 and
342 LF210, respectively, but only by 36% from LF240. The fraction of SCOD not removed
343 from LFs can be assigned to refractory compounds formed during the hydrothermal
344 treatment as previously found by Villamil et al. (2018) in the anaerobic digestion of LF
345 from sewage sludge. SCOD removed from MAB corresponded to extracellular SCOD
346 available in the reaction medium. However, the fact that no increase in SCOD
347 concentration was observed during digestion suggests that no MAB was hydrolyzed. As
348 can be seen from Fig. 3b, the TVFA concentration increased over the first few days by
349 effect of the hydrolytic–acidogenic stage in all runs. Then, the concentration decreased
350 by up to 53 and 32% with LF180 and LF210, respectively. On the other hand, the TVFA
351 concentration in LF240 increased gradually to approximately 780 mg COD L^{-1}. These
352 results are consistent with the trends in SCOD removal. VFA accumulation in the digester
353 is an indicator of instability resulting from the production and elimination reactions being
354 uncoupled. In this situation, methanogens are unable to remove volatile organic acids fast
355 enough and imbalances in biogas production result (Appels et al., 2008). On the other
356 hand, changes in the TVFA concentration were virtually negligible with MAB. A meager
357 VFA production/uptake ratio thus resulted that testifies to the resistance of the cell
358 envelope to biological degradation.
359
360 The anaerobic digestion of MAB produces biogas by degradation of organic matter in
361 cells as a result of solar energy being used for photosynthesis. The methane yield obtained
362 by AD of MAB in this work (Fig. 3c), 120 ± 5 mL STP CH_4 g^{-1} VS_{added}, was much lower
363 than the theoretical value based on its composition (carbohydrates, lipids and proteins)
364 (Guiot and Frigon, 2012), but similar than that obtained by Passos et al. (2014) and Tran
365 et al. (2014) (100–130 mL STP CH_4 g^{-1} VS_{added}) by digesting mixed cultures. The low
366 biodegradability of our material was a result of the structural integrity of cell walls, which
367 was in turn a function of the biochemical composition and/or physicochemical properties.
368 The high resistance of cell walls to disruption may somehow have hindered extraction of
369 intracellular material, thereby also reducing the release of more easily degradable matter

370 and leading to increased methane yields. The HTC process facilitates cell disruption and
371 hence the release of volatile matter for valorization by anaerobic digestion. A lag-phase
372 spanning the first 3–5 days in each run was observed in all substrates suggesting that the
373 inoculum required some time to adapt to the substrate. Thereafter, methane yield
374 increased exponentially as a result of VFA uptake by methanogenic *Archaea*. In general,
375 the liquid fractions exhibited greater anaerobic biodegradability than raw MAB. Thus,
376 the final methane yields obtained from LF180, LF210 and LF240 were 356 ± 12, 226 ±
377 3, and 188 ± 8 mL STP CH_4 g^{-1} VS_{added}, and hence 1.5–3 times higher than MAB.
378
379 *3.4. Analysis of refractory compounds*
380 Figure 4 shows the semi-quantitative composition of LF180, LF210 and LF240 before
381 and after anaerobic digestion. The compounds studied clustered into chemical groups and
382 their composition was expressed in terms of % peak area. Raising the HTC temperature
383 reduced the diversity of oxygenated hydrocarbons species in LFs. Aldehydes (e.g., 2-
384 methyl pentanal, benzaldehyde and glutaraldehyde) and esters such as methylethyl
385 formate were detected in LF180 but not when the HTC temperature was raised above 210
386 ºC. Rather, the concentrations of aromatic hydrocarbons increased with increasing
387 temperature from 180 to 210 ºC and then decreased upon further raising to 240 ºC. The
388 different HTC conditions resulted in an also different aromatic hydrocarbon composition.
389 Anaerobic digestion caused complete removal of aldehydes and esters from LF180, and
390 partial removal of aromatic hydrocarbons from LF210 and LF240. Villamil et al. (2018)
391 previously accomplished nearly complete removal of aldehydes produced by HTC of
392 sewage sludge at 210 ºC with AD of the aqueous phase. However, some aromatic
393 compounds such as phenol, 2,3,5,6-tetramethyl benzene, 2-methylpropyl cyclohexane
394 were refractory to AD and accounted for 52% of the total composition of LF180 upon
395 digestion.
396
397 On the other hand, raising the HTC temperature expanded the diversity of nitrogenated
398 species in the liquid fractions. The nitrogen-containing species in LF180 were ring-type

399 structures with two N heteroatoms such as pyrimidine and pyrazines that formed mainly
400 through hydrolysis of proteins (Costanzo et al., 2015). Increasing the HTC temperature
401 above 210 ºC led to compounds with one or two N heteroatoms (e.g., pyrroles, indole,
402 amines) being present in LFs alongside other nitrogenated aromatic compounds formed
403 in Maillard-type reactions (Broch et al., 2014). The fact that LF240 contained indole,
404 which can be degraded by methanogens and sulfate-reductive microbial populations
405 (Fisher et al., 2017), suggests terminal process inhibition as a result of poor digestion.
406 Anaerobic digestion efficiently removed most of the pyrimidines formed at HTC
407 temperatures below 240 ºC. Likewise, the nitrogenous species accounting for residual
408 SCOD in LF240 may have inhibited methanogens through accumulation of VFA
409 intermediates.
410
411 *3.5. Energy recovery*
412 Figure 5 shows the amount of energy produced per kg dry feedstock and the percent net
413 energy recovery for the valorization of MAB by conventional anaerobic digestion and the
414 HTC–AD combination. The energy produced from MAB by conventional AD is limited
415 owing to the low methane yield resulting from the also low degradability of the organic
416 fraction —usually less than 34–50% (Ras et al., 2011; Xia et al., 2013). Keymer et al.
417 (2013) found a high-pressure thermal hydrolysis pretreatment to increase methane yields
418 by up to 81% as a result of its increasing the SCOD fraction above 50%. HTC provides
419 an alternative for improved valorization of MAB by recovering energy through hydrochar
420 and methane formed by anaerobic digestion of the liquid fraction.
421
422 The HHV for MAB obtained in this work, 16.9 MJ kg^{-1}, was taken to be the total amount
423 of energy stored in the feedstock (see Table 1). Anaerobic digestion of raw MAB provided
424 4.0 MJ per kg dry feedstock, which was only 20% of the net amount stored in MAB. The
425 HTC180 treatment in combination with anaerobic digestion of LF180 provided the largest
426 amount of energy (15.4 MJ per kg dry feedstock, which accounted for 91% of the net
427 amount of energy stored in MAB). By contrast, HTC210 + AD of LF210 provided 12.1

MJ per kg dry feedstock (viz., 72% of the total amount of energy), and HTC240 + AD of LF240 provided 10.4 MJ per kg dry feedstock (62% of the total energy storage). An increased HTC temperature therefore reduced net energy recovery, possibly because of the low HHV of hydrochar and the poor biodegradability of the liquid fraction by effect of carbon losses and formation of refractory compounds at relative high HTC temperatures. Thus, using the lowest HTC temperature (180 ºC) is recommended to substantially improve the valorization of MAB by HTC–AD.

4. Conclusions

Hydrothermal carbonization of microalgal biomass provided hydrochars and a spent liquor with a high content in organic matter that can be valorized by anaerobic digestion. Processing microalgae at 180 °C provided a hydrochar with significantly lower H/C and O/C atomic ratios than lignite in addition to a similar higher heating value. The energy recovery obtained by anaerobic digestion of the liquid fraction, in combination with the energy content of the hydrochar, allows the amount of energy produced by conventional anaerobic digestion of microalgal biomass to be increased 3.85 times. Therefore, a combined HTC–AD treatment provides a seemingly effective method for valorizing microalgal biomass.

Acknowledgements

The authors wish to express their gratitude to Spain's MINECO (CTM2016-76564-R and RYC-2013-12549) for funding this work, and to A. Vilar and B. Villajos for their valuable help.

References

1. American Public Health Association/American Water Works Association/Water Environment Federation (APHA, AWWA, WEF), Standard Methods for the Examination of Water and Wastewater, 20th ed. 1998. Washington, DC.
2. Appels, L., Baeyens, J., Degre, J., Dewil, R., 2008. Principles and potential of the

457 anaerobic digestion of waste-activated sludge. Prog. Energ. Combust. 34, 755–
458 781.
459 3. Aragón-Briceño, C., Ross, A.B., Camargo-Valero M.A., 2017. Evaluation and
460 comparison of product yields and bio-methane potential in sewage digestate
461 following hydrothermal treatment. Appl. Energy 208, 1357–1369.
462 4. Ayala-Parra, P., Liu, Y., Field, J.A., Sierra-Alvarez, R., 2017. Nutrient recovery
463 and biogas generation from the anaerobic digestion of waste biomass from algal
464 biofuel production. Renew. Energy 108, 410–416.
465 5. Barbera, E., Bertucco, A., Kumar, S., 2018. Nutrients recovery and recycling in
466 algae processing for biofuels production. Renew. Sustain. Energy Rev. 90, 28–42.
467 6. Broch, A., Jena, U., Hoekman, S.K., Langford, J., 2014. Analysis of solid and
468 aqueous phase products from hydrothermal carbonization of whole and lipid-
469 extracted algae. Energies 7, 62–79.
470 7. Chiaramonti, D., Prussi, M., Buffi, M., Rizzo, A.M., Pari, L., 2017. Review and
471 experimental study on pyrolysis and hydrothermal liquefaction of microalgae for
472 biofuel production. Appl. Energy 185, 963–972.
473 8. Costanzo, W., Jena, U., Hilten, R., Das, K.C., Kastner, J.R., 2015. Low
474 temperature hydrothermal pretreatment of algae to reduce nitrogen heteroatoms
475 and generate nutrient recycle streams. Algal Res. 12, 377–387.
476 9. De la Rubia, M.A., Villamil J.A., Rodriguez J.J., Mohedano A.F., 2018a. Effect
477 of inoculum source and initial concentration on the anaerobic digestion of the
478 liquid fraction from hydrothermal carbonisation of sewage sludge. Renew. Energ.
479 127, 697–704.
480 10. De la Rubia, M.A., Villamil, J.A., Rodriguez, J.J., Borja, R., Mohedano, A.F.,
481 2018b. Mesophilic anaerobic co-digestion of the organic fraction of municipal
482 solid waste with the liquid fraction from hydrothermal carbonization of sewage
483 sludge. Waste Manage. 76, 315–322.

484 11. Delrue, F., Setier, P-A., Sahut, C., Cournac, L., Roubaud, A., Peltier, G., Froment,
485 A-K., 2012. An economic, sustainability, and energetic model of biodiesel
486 production from microalgae. Bioresour. Technol. 111, 191–200.
487 12. Dubois, F., Gilles, M., Hamilton, K.A., Rebers, J.K., Smith, P.A. 1956.
488 Colorimetric method for determination of sugars and related substances. Anal.
489 Chem. 28, 350–356.
490 13. Ekpo, U., Ross, A.B., Camargo-Valero, M.A., Williams, P.T., 2016. A
491 comparison of product yields and inorganic content in process streams following
492 thermal hydrolysis and hydrothermal processing of microalgae, manure and
493 digestate. Bioresour. Technol. 200, 951–960.
494 14. Engin, B., Atakül, H., Ünlü, A., Olgun, Z., 2018. CFB combustion of low-grade
495 lignites: Operating stability and emissions. J. Energy Inst. DOI:
496 10.1016/j.joei.2018.04.004.
497 15. Fasaei, F., Bitter, J.H., Slegers, P.M., van Boxtel, A.J.B., 2018. Techno-economic
498 evaluation of microalgae harvesting and dewatering systems. Algal Res. 31, 347–
499 362.
500 16. Fisher, R.M., Le-Minh, N., Sivret, E.C., Alvarez-Gaitan, J.P., Moore, S.J., Stuetz,
501 R.M., 2017. Distribution and sensorial relevance of volatile organic compounds
502 emitted throughout wastewater biosolids processing. Sci. Total Environ. 599–600,
503 663–670.
504 17. Funke, A., Ziegler, F., 2010. Hydrothermal carbonization of biomass: a summary
505 and discussion of chemical mechanisms for process engineering. Biofuels
506 Bioprod. 4, 160–177.
507 18. Gouveia, L., Graça, S., Sousa, C., Ambrosano, L., Ribeiro, B., Botrel, L.P., Castro
508 Neto, P., Ferreira, A.F., Silva, C.M., 2016. Microalgae biomass production using
509 wastewater: Treatment and costs scale-up considerations. Algal Res. 16, 167–176.
510 19. Guiot, S.R., Frigon, J-C., 2012. Anaerobic digestion as an effective biofuel
511 production technology in Hallenbeck, P.C. (Ed.). Microbial Technologies in
512 Advanced Biofuels Production, Springer, pp. 143–161

513 20. Guldhe, A., Singh, B., Rawat, I., Ramluckan, K., Bux, F., 2014. Efficacy of drying
514 and cell disruption techniques on lipid recovery from microalgae for biodiesel
515 production. Fuel 128, 46–52.
516 21. He, C., Giannis, A., Wang, J., 2013. Conversion of sewage sludge to clean solid
517 fuel using hydrothermal carbonization: Hydrochar fuel characteristics and
518 combustion behavior. Appl. Energy 111, 257–266.
519 22. Heilmann, S.M., Davis, H.T., Jader, L.R., Lefebvre, P.A., Sadowsky, M.J.,
520 Schendel, F.J., von Keitz, M.G., Valentas, K.J. 2010. Hydrothermal carbonization
521 of microalgae. Biomass Bioenerg. 34, 875–882.
522 23. Hernández, D., Riaño, B., Coca, M., García-González, M.C., 2013. Treatment of
523 agro-industrial wastewater using microalgae–bacteria consortium combined with
524 anaerobic digestion of the produced biomass. Bioresour. Technol. 135, 598–603.
525 24. Hernández, D., Molinuevo-Salces, B., Riaño, B., Larrán-García, A.M., Tomás-
526 Almenar, C., García-González, M.C., 2018. Recovery of protein concentrates
527 from microalgal biomass grown in manure for fish feed and valorization of the
528 byproducts through anaerobic digestion. Front. Sustain. Food Syst. 2:28. DOI:
529 10.3389/fsufs.2018.00028.
530 25. Hosseinizand, H., Lim C.J., Webb, E., Sokhansanj, S., 2017. Economic analysis
531 of drying microalgae *Chlorella* in a conveyor belt dryer with recycled heat from
532 a power plant. Appl. Thermal Eng. 124, 525–532.
533 26. Ho, S-H., Huang, S-W., Chen, C-Y., Hasunuma, T., Kondo, A., Chang, J-S., 2013.
534 Bioethanol production using carbohydrate-rich microalgae biomass as feedstock.
535 Bioresour. Technol. 135, 191–198.
536 27. Keymer, P., Ruffell, I., Pratt, S., Lant, P., 2013. High pressure thermal hydrolysis
537 as pre-treatment to increase the methane yield during anaerobic digestion of
538 microalgae. Bioresour. Technol. 131, 128–133.
539 28. Lee, C.S., Oh, H-S., Oh, H-M., Kim, H-S., Ahn, C.Y., 2016. Two-phase
540 photoperiodic cultivation of algal–bacterial consortia for high biomass production

541 and efficient nutrient removal from municipal wastewater. Bioresour. Technol.
542 200, 867–875.
543 29. Lee, J., Lee, K., Sohn, D., Kim, Y.M., Park, K.Y., 2018. Hydrothermal
544 carbonization of lipid extracted algae for hydrochar production and feasibility of
545 using hydrochar as a solid fuel. Energy 153, 913–920.
546 30. López Barreiro, D., Samorì, C., Terranella, G., Hornung, U., Kruse, A., Prins, W.,
547 2014. Assessing microalgae biorefinery routes for the production of biofuels via
548 hydrothermal liquefaction. Bioresour. Technol. 174, 256–265.
549 31. Missaoui, A., Bostyn, S., Belandria, V., Cagnon, B., Sarh, B., Gökalp, I., 2017.
550 Hydrothermal carbonization of dried olive pomace: Energy potential and process
551 performances. J. Anal. Appl. Pyrolysis 128, 281–290.
552 32. Nuchdang, S., Frigon, J-C., Roy, C., Pilon, G., Phalakornkule, C., Guiot, S.R.,
553 2018. Hydrothermal post-treatment of digestate to maximize the methane yield
554 from the anaerobic digestion of microalgae. Waste Manage. 71, 683–688.
555 33. Park, K.Y., Lee, K., Kim, D., 2018. Characterized hydrochar of algal biomass for
556 producing solid fuel through hydrothermal carbonization. Bioresour. Technol.
557 258, 119–124.
558 34. Passos, F., Uggetti, E., Carrère, H., Ferrer, I., 2014. Pre-treatment of microalgae
559 to improve biogas production: a review. Bioresour. Technol. 172, 403–412.
560 35. Puccini, M., Ceccarini, L., Antichi, D., Seggiani, M., Tavarini, S., Hernandez
561 Latorre, M., Vitolo, S., 2018. Hydrothermal carbonization of municipal woody
562 and herbaceous prunings: hydrochar valorisation as soil amendment and growth
563 medium for horticulture. Sustainability 10, 846. DOI:10.3390/su10030846.
564 36. Randall, R.J., Lewis, A., 1951. The folin by oliver. Readings, 93, 265–275.
565 37. Raposo, F., de la Rubia, M.A., Borja, R., Alaiz, M., 2008. Assessment of a
566 modified and optimised method for determining chemical oxygen demand of solid
567 substrates and solutions with high suspended solid content. Talanta 76, 448–453.

568 38. Ras, M., Lardon, L., Bruno, S., Bernet, N., Steyer, J.P., 2011. Experimental study
569 on a coupled process of production and anaerobic digestion of *Chlorella vulgaris*.
570 Bioresour. Technol. 102, 200–206.
571 39. Santos, F.M., Pires, J.C.M., 2018. Nutrient recovery from wastewaters by
572 microalgae and its potential application as bio-char. Bioresour. Technol. 267,
573 725–731.
574 40. Shurtz, B.K., Wood, B., Quinn, J.C., 2017. Nutrient resource requirements for
575 large-scale microalgae biofuel production: Multi-pathway evaluation. Sust.
576 Energ. Technol. Assess. 19, 51–58.
577 41. Smith, A.M., Whittaker, C., Shield, I., Ross, A.B., 2018. The potential for
578 production of high quality bio-coal from early harvested *Miscanthus* by
579 hydrothermal carbonization. Fuel 220, 546–557.
580 42. Tran, K.C., Mendoza Martin, J.L., Heaven, S., Banks, C.J., Acien Fernandez,
581 F.G., Molina Grima, E., 2014. Cultivation and anaerobic digestion of
582 *Scenedesmus* spp. grown in a pilot-scale open raceway. Algal Res. 5, 95–102.
583 43. Villamil, J.A., Mohedano, A.F., Rodriguez, J.J., de la Rubia, M.A., 2018.
584 Valorisation of the liquid fraction from hydrothermal carbonisation of sewage
585 sludge by anaerobic digestion. J. Chem. Technol. Biotechnol. 93, 450–456.
586 44. Villamil, J.A., Mohedano, A.F., Rodriguez, J.J., de la Rubia, M.A., 2019.
587 Anaerobic co-digestion of the aqueous phase from hydrothermally treated waste
588 activated sludge with primary sewage sludge. A kinetic study. J. Environ.
589 Manage. 231, 726–733.
590 45. Wang, T., Zhai, Y., Zhu, Y., Peng, C., Xu, B., Wang, T., Li, C., Zeng, G., 2018.
591 Influence of temperature on nitrogen fate during hydrothermal carbonization of
592 food waste. Bioresour. Technol. 247, 182–189.
593 46. Xia, A., Cheng, J., Ding, L., Lin, R., Huang, R., Zhou, J., Cen, K., 2013.
594 Improvement of the energy conversion efficiency of *Chlorella pyrenoidosa*
595 biomass by a three-stage process comprising dark fermentation,
596 photofermentation, and methanogenesis. Bioresour. Technol. 146, 436–443.

47. Yao, C., Wu, P., Pan, Y., Lu, H., Chi, L., Meng, Y., Cao, X., Xue, S., Yang, X., 2016. Evaluation of the integrated hydrothermal carbonization–algal cultivation process for enhanced nitrogen utilization in *Arthrospira platensis* production. Bioresour. Technol. 216, 381–390.

48. Yu, G., Zhang, Y., Guo, B., Funk, T., Schideman, L., 2014. Nutrient flows and quality of bio-crude oil produced via catalytic hydrothermal liquefaction of low-lipid microalgae. Bioenerg. Res. 7, 1317–1328.

Table 1. Representative analysis of microalgal biomass and hydrochars.

	MAB	**HC180**	**HC210**	**HC240**
C (%)	38.4 ±0.3	40.7 ±0.3	41.8 ±0.9	38.8 ±0.3
H (%)	5.3 ± 0.1	5.3 ± 0.1	5.1 ± 0.1	4.7 ± 0.1
N (%)	5.8 ± 0.1	4.3 ± 0.1	3.7 ± 0.3	2.3 ± 0.1
S (%)	0.5 ± 0.1	0.1 ± 0.1	0.2 ± 0.1	0.1 ± 0.1
O (%)	20.3 ±0.2	14.9 ±0.1	9.8 ±0.2	8.3 ±0.1
Volatile matter (%)	48.3 ±0.2	45.9 ±0.1	40.4 ±0.2	34.0 ±0.1
Fixed carbon (%)	12.1 ±0.3	10.9 ±0.1	12.0 ±0.2	13.4 ±0.1
Ash (%)	29.7 ±0.2	34.7 ±0.2	39.5 ±0.2	45.7 ±0.3
HHV (MJ kg^{-1})	16.9 ±0.1	18.0 ±0.1	18.6 ±0.1	16.7 ±0.1

Table 2. Effect of hydrochar treatment on elemental composition.

	C (%)	H (%)	N (%)	S (%)
HC 210	41.8 ± 0.9	5.1 ± 0.1	3.7 ± 0.3	0.2 ± 0.1
HC 210 (H_2O_2)	26.0 ± 0.5	4.3 ± 0.1	2.3 ± 0.1	0.1 ± 0.1
HC 210 (EtOH)	41.6 ± 0.3	4.6 ± 0.1	5.8 ± 0.1	0.2 ± 0.1
HC 210 (HCl)	58.6 ± 0.2	6.3 ± 0.1	6.9 ± 0.1	0.2 ± 0.1

Table 3. Characterization of microalgal biomass (MAB) and liquid fractions (LFs) obtained after HTC at 180, 210 and 240 ºC.

	MAB	**LF180**	**LF210**	**LF240**
Total solids (g L^{-1})	65.9 ± 3.5	34.8± 0.7	26.5± 0.6	25.1± 0.8
Volatile solids (g L^{-1})	57.9 ± 2.5	33.8± 0.5	24.5± 0.6	23.1 ± 0.8
Soluble chemical oxygen demand (g L^{-1})	2.5 ± 0.2	26.8 ± 0.4	22.3 ± 0.0	22.8 ± 0.6
Soluble carbohydrates (g L^{-1})	0.6 ± 0.0	3.7 ± 0.1	1.2 ± 0.2	0.5 ± 0.0
Soluble proteins (g L^{-1})	1.3 ± 0.1	9.9 ± 0.3	8.4 ± 0.1	7.5 ± 0.7
pH	5.7 ± 0.1	6.1 ± 0.1	6.4 ± 0.1	6.7 ± 0.1
Total alkalinity (g $CaCO_3$ L^{-1})	2.3 ± 0.1	3.8 ± 0.1	3.8 ± 0.1	5.1 ± 0.1
Total volatile fatty acids (g COD L^{-1})	3.1 ± 0.7	1.4 ± 0.8	1.5 ± 0.1	2.9 ± 0.3
Total organic carbon (TOC) (g L^{-1})	2.4 ± 0.1	12.8 ± 0.1	11.5 ± 0.1	13.1 ± 0.1

Figure captions

Figure 1. van Krevelen diagram for microalgal biomass and hydrochars obtained from MAB and from activated sludge.

Figure 2. Elementary content in microalgal biomass and hydrochars.

Figure 3. Time-course of total soluble chemical oxygen demand (a), volatile fatty acids (b), and cumulative methane yield (c) during anaerobic batch assays of MAB and LFs.

Figure 4. GC/MS analysis of chemical species in LF180 (a), LF210 (b), LF240 (c) samples, before (fulfill) and after (strings) AD assay.

Figure 5. Energy produced and net energy recovery for the valorization of microalgal biomass using conventional AD and HTC coupled with AD.

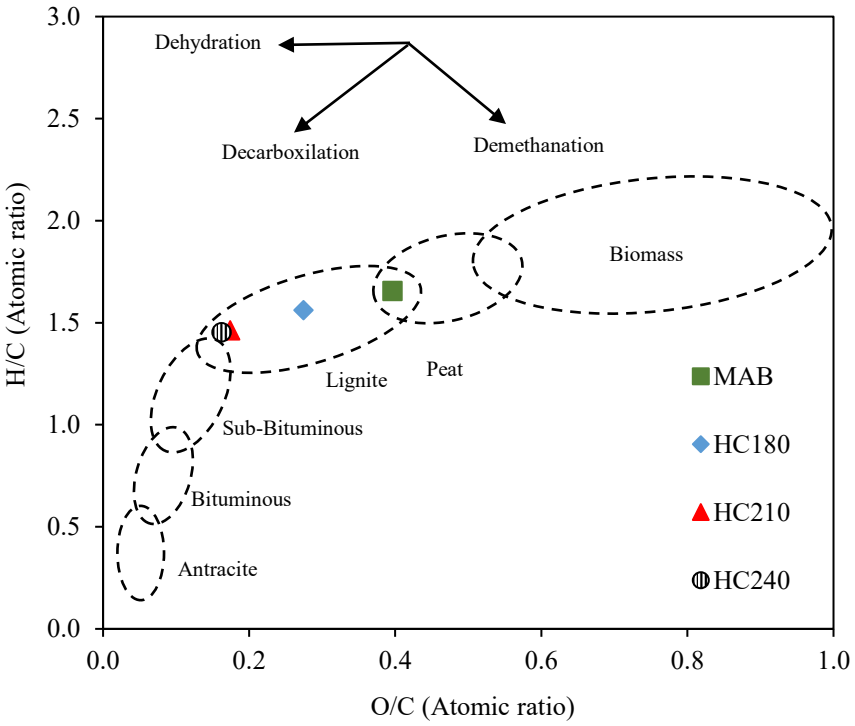

Figure 1. van Krevelen diagram for microalgal biomass and hydrochars obtained from MAB and from activated sludge.

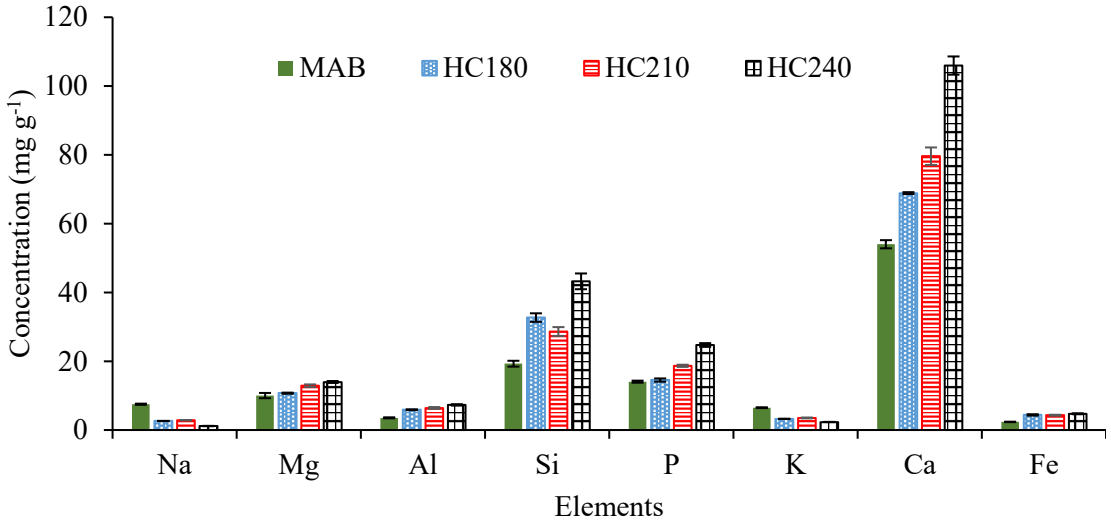

Figure 2. Elementary content in microalgal biomass and hydrochars

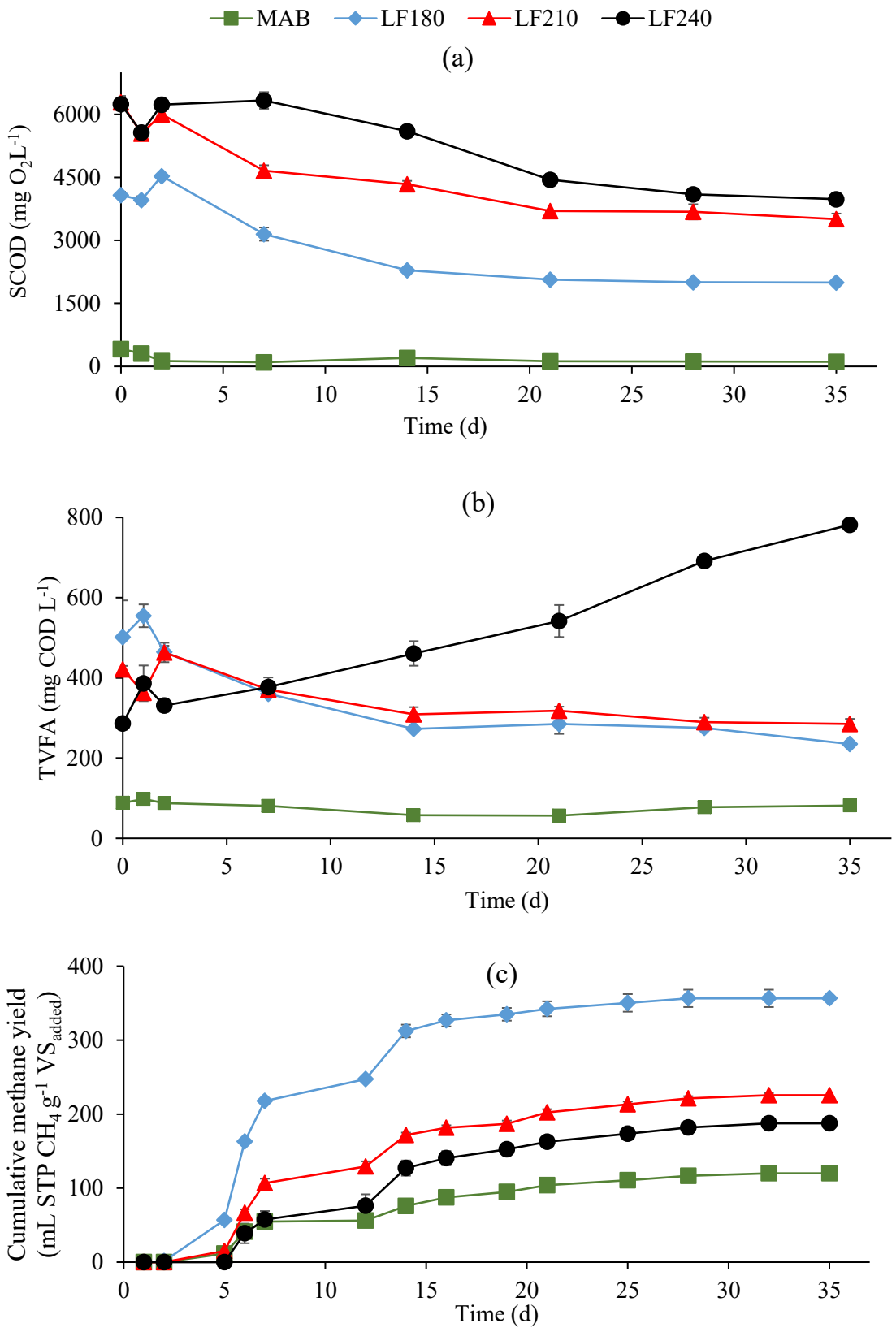

Figure 3. Time-course of total soluble chemical oxygen demand (a), total volatile fatty acids (b), and cumulative methane yield (c) during anaerobic batch assays of MAB and LFs.

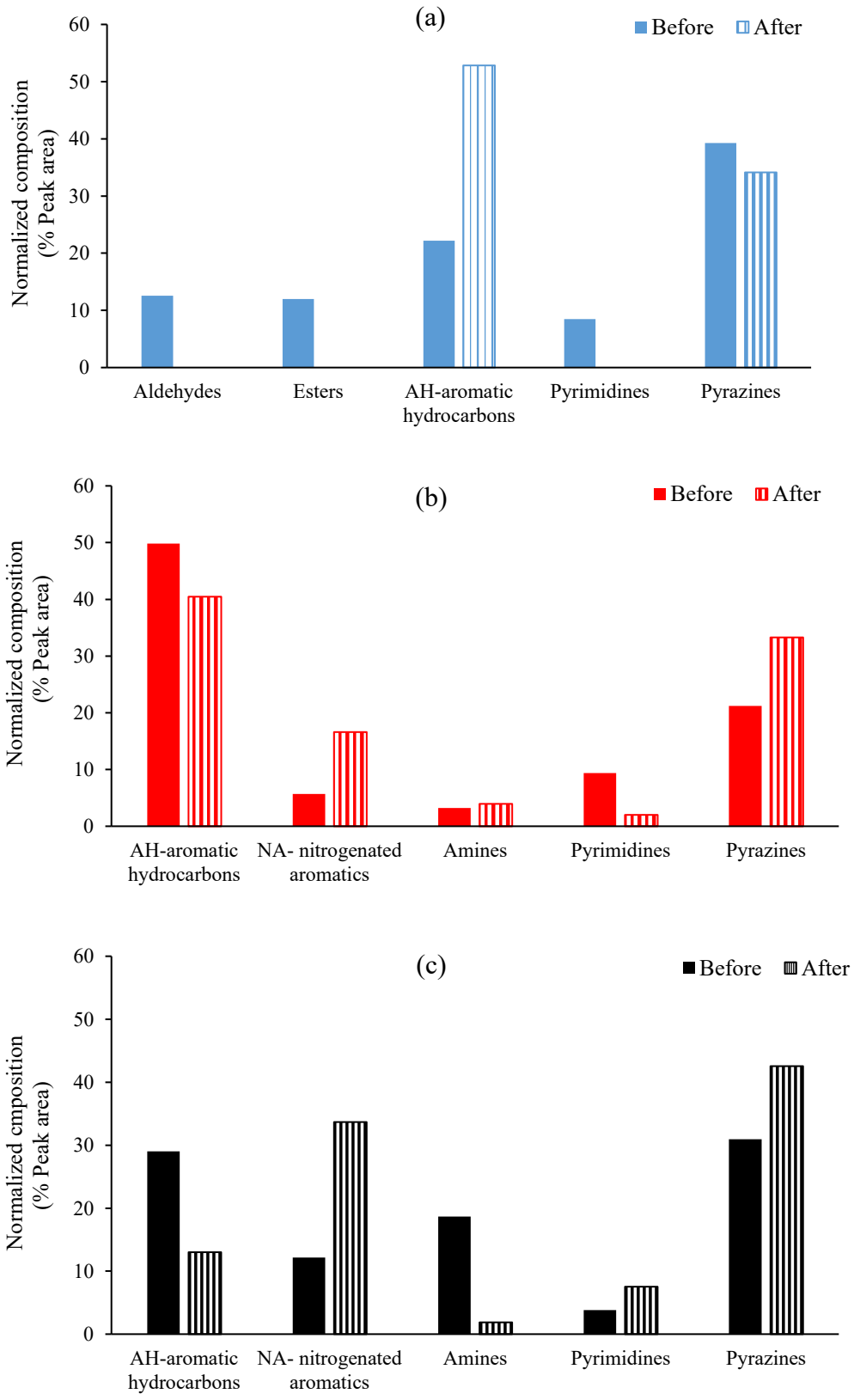

Figure 4. GC/MS analysis of chemical species in LF180 (a), LF210 (b), LF240 (c) samples, before (fulfill) and after (strings) AD assay.

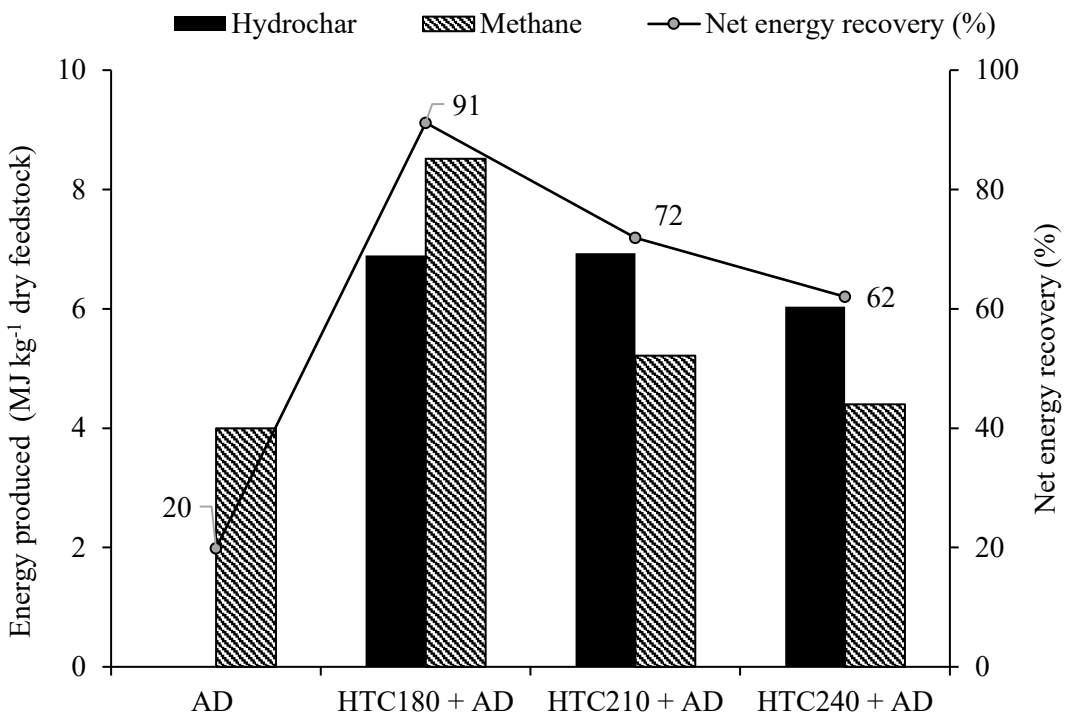

Figure 5. Energy produced and net energy recovery for the valorization of microalgal biomass using conventional AD and HTC coupled with AD.